Eye (2012) 26, 1086–1094

www.nature.com/eye

CLINICAL STUDY

Tomographic fundus features in pseudoxanthoma elasticum: comparison with neovascular age-related macular degeneration in Japanese patients

AA Ellabban[1,2], M Hangai[1], K Yamashiro[1], S Nakagawa[1], A Tsujikawa[1] and N Yoshimura[1]

Abstract

Purpose **To determine the retinal and subretinal features characteristic to pseudoxanthoma elasticum (PXE) compared with age-related macular degeneration by using spectral-domain optical coherence tomography (SD-OCT) in Japanese patients.**
Methods **We reviewed colour fundus photographs, fluorescein angiograms, and SD-OCT images of 52 eyes (27 Japanese patients) with angioid streaks (AS) due to PXE. Then we compared the incidence of tomographic features between 24 eyes (24 patient) with choroidal neovascularization (CNV) secondary to AS and 44 eyes (44 patients) with CNV secondary to age-related macular degeneration (AMD).**
Results **Secondary CNV was found in 44 eyes (84.6%) of 52 patients with PXE during follow-up. We found characteristic round or ovoid tubular structures with highly reflective annular lines (termed 'outer retinal tubulation' (ORT)) in 31 (70.5%) of 44 eyes with CNV, but none were found in eyes without CNV. We also found characteristic undulations of Bruch's membrane in 38 (73.1%) eyes with AS. The incidence of ORT was significantly greater in eyes with CNV secondary to AS (70.8%; $P = 0.005$) compared with eyes with CNV secondary to AMD (34.1%). The incidence of Bruch's membrane undulation was significantly greater in eyes with CNV secondary to AS (70.8%; $P < 0.0001$) than in eyes with CNV secondary to AMD (11.4%).**
Conclusion **SD-OCT imaging clearly revealed a greater incidence of unique lesions, including ORT and Bruch's membrane undulation, in eyes in PXE patients with CNV secondary to AS than in eyes with CNV secondary to AMD.**
Eye (2012) **26,** 1086–1094; doi:10.1038/eye.2012.101; published online 1 June 2012

Keywords: pseudoxanthoma elasticum; angioid streaks; age-related macular degeneration; spectral-domain optical coherence tomography

[1]Department of Ophthalmology and Visual Sciences, Kyoto University Graduate School of Medicine, Kyoto, Japan

[2]Department of Ophthalmology, Suez Canal University, Ismailia, Egypt

Correspondence:
M Hangai, Department of Ophthalmology and Visual Sciences, Kyoto University Graduate School of Medicine, 54 Kawahara-cho, Shougoin, Sakyo-ku, Kyoto 606-8507, Japan
Tel: +81-75-751-3259;
Fax: +81-75-752-0933.
E-mail: hangai@kuhp.kyoto-u.ac.jp

Received: 26 January 2012
Accepted in revised form: 15 April 2012
Published online: 1 June 2012

Introduction

Pseudoxanthoma elasticum (PXE) is a rare systemic disease, affecting 1 in 25 000–100 000 people; it mainly affects the cardiovascular system, skin, and eyes with a variable phenotype.[1] This disorder is a consequence of mutations in the ABCC6 gene.[2,3] The progressive fragmentation and calcification of elastic fibres in connective tissue result in pathological changes that are most pronounced in the dermis, Bruch's membrane, and blood vessels.[1,3] Characteristic lesions at the fundus are angioid streaks (AS), peau d'orange, areas of chorioretinal atrophy, and secondary choroidal neovascularization (CNV).[1,3] Although this disorder is rare, it leads to severe vision loss when CNV develops.[4,5]

AS occurs as irregular crack-like dehiscence in the Bruch's membrane. These cracks in the Bruch's membrane allow the ingrowth of the

CNV into the subretinal space.[6] Although AS may occur in isolation or as ocular manifestations of systemic diseases, such as Paget's disease, acromegaly, or Ehlers–Danlos syndrome, the most common disease related to AS is PXE.[7–9]

CNVs secondary to AS occur in 72–86% of AS-affected eyes, are bilateral in more than 70% of cases, and tend to affect middle-aged patients. They lead to poor visual prognosis, especially when the CNV involves the macular area.[6,8,10–12] The efficacy of various treatment modalities, including laser photocoagulation, transpupillary thermotherapy, PDT with verteporfin, and rarely macular translocation, is limited and even worse in eyes with CNV secondary to AS compared with those secondary to AMD (age-related macular degeneration).[7,9,13–18] It is useful to identify the differences in the fundus lesions that underline the different responses to treatment between these diseases.

Spectral-domain optical coherence tomography (SD-OCT) technology allows cross-sectional imaging to an almost histological level by effective reduction of speckle noise, thus allowing the visualization of retinal microstructural abnormalities *in vivo*.[19,20] Recent studies[21,22] reported unique tomographic features on SD-OCT in eyes with AS, such as breaks in Bruch's membrane, alternating reflectivity within Bruch's membrane associated with Peau d'orange, outer retinal tabulation (ORT),[23] and subretinal granular appearance associated with the pattern dystrophy-like changes on fluorescein angiograms and autofluorescence. However, the comparison of SD-OCT findings between eyes with AS and AMD has not been reported.

The purpose of this study is to show the characteristics of AS lesions by comparing SD-OCT features in eyes with CNV secondary to AS associated with PXE with those secondary to AMD by using speckle noise-reduced SD-OCT imaging.

Materials and methods

We conducted a retrospective study of consecutive patients with PXE who were examined by SD-OCT at Kyoto University Hospital from January 2008 to May 2010. All patients underwent complete ophthalmic examination including best-corrected visual acuity using the 5-m Landolt chart, intraocular pressure measurements using a Goldmann applanation tonometer, slit-lamp examinations, fundus examination with colour fundus photography (Topcon TRC50LX; Topcon, Tokyo, Japan), indirect ophthalmoscopy, and slit-lamp biomicroscopy. Fluorescein angiography (FA), indocyanine green angiography, and SD-OCT were performed simultaneously by using a Spectralis HRA + OCT (Heidelberg Engineering, Heidelberg, Germany). Patient data were collected through a review of our medical records. All investigations of this study adhered to the tenets of the Declaration of Helsinki. This study was approved by the Institutional Review Board and Ethics Committee of the Kyoto University Graduate School of Medicine. Informed consent was obtained for all patients.

The diagnosis of PXE was based on characteristic systemic manifestation including fundus findings in photographs as well as FA as described by Shields *et al*.[11] The diagnosis was then further confirmed by characteristic histopathological abnormalities in skin biopsy. Eyes with opaque media (eg, cataracts) and vitreous haemorrhage were excluded from analysis.

SD-OCT imaging

SD-OCT imaging was performed for all patients by using a Spectralis HRA + OCT system with automated eye tracking and image alignment modules. The software allows the averaging of up to 100 single B-scan images from the same location of interest in real time (automatic real-time 'ART' module). This enables effective speckle noise reduction, which markedly improves the visualization of retinal layer boundaries and the borders of various pathological lesions to help reveal the detailed structures of various pathologies.[19–22]

Our routine SD-OCT examination, using this instrument, included 6- or 9-mm radial macular scans, and 6- or 9-mm horizontal and vertical serial scans for the entire macular area. In each scan, 50 B scans were averaged to reduce speckle noise.

Comparative studies of eyes with CNV secondary to AS and AMD

We compared the incidence of characteristic tomographic features between eyes with CNV secondary to AS and AMD. All of the patients with AS who had CNV were included in this comparison. Control eyes with CNV secondary to AMD were randomly selected from patient pools in Kyoto University Hospital from January 2008 to May 2010. When both eyes in a single patient were eligible for this comparison, one eye was selected randomly.

Statistics

Statistical analysis was performed using the SPSS statistical software (version 16; SPSS Inc., Chicago, IL, USA). Fisher's exact test was used to analyse categorical variables (gender, incidence of ORT, cystoid spaces, Bruch's membrane undulation, serous retinal

detachment (SRD), and locations of ORT). Unpaired *t*-tests were used to compare numerical variables (age, refraction, best-corrected visual acuity, SD-OCT follow-up period, and the number of SD-OCT examinations). Best-corrected visual acuity was converted to the logarithm of the minimum angle of resolution (LogMAR) for statistical analysis. *P*-values less than 0.05 were considered statistically significant.

Results

A total of 52 eyes from 27 patients (17 males and 10 females) were included in this retrospective study. All patients were Japanese (Table 1). Their mean age was 65.8 (SD, 10.1) years (range, 50–89 years). The mean follow-up time was 39.5 (18.8) months (range, 3–61 months). The mean follow-up period by SD-OCT was 12.6 (9.6) months (range, 1–27 months). The mean number of SD-OCT examinations per patient was 4.1 (3.1) (range, 1–13 examinations). Two eyes from two patients were excluded due to the presence of vitreous haemorrhage and cataract in one eye each. Seven eyes with AS were excluded because of poor SD-OCT image quality.

All 27 patients exhibited systemic manifestations of PXE, including characteristic skin and fundus lesions. In all, 26 patients (96.3%) were diagnosed with PXE on the basis of skin biopsy results (skin biopsy was not performed for 1 patient).

Biomicroscopic and angiographic findings

Angioid streaks were seen in all of the 52 eyes, and Peau d'orange were observed in 50 (96.2%) eyes. No eyes showed the pattern dystrophy-like changes on fluorescein angiogram or optic nerve head drusen.

Secondary CNV was found in 44 eyes (84.6%) of 52 eyes with PXE by FA at the initial examination. No other eyes developed CNV during the follow-up as observed by SD-OCT. SRD was only found in 7 eyes (13.5%) when observed using SD-OCT.

Of the 44 eyes with secondary CNV, 26 (59.1%) eyes had a history of treatment for CNV before the beginning of SD-OCT follow-up (successive PDT and anti-VEGF for 14 eyes, anti-VEGF therapy only for 5 eyes, and photodynamic therapy only for 7 eyes) and 16 (36.4%) eyes received treatment during the follow-up by SD-OCT (anti-VEGF therapy only for 8 eyes and combined photodynamic and anti-VEGF therapies for 8).

Tomographic findings in eyes with AS

Outer retinal tabulation. Incidence and morphology: We found that there were characteristic round or ovoid tubular structures in the outer retina in 31 (59.6%) of 52 eyes (Table 1). These structures were nearly same as those reported to be 'outer retinal tubulation' (ORT) found primarily in eyes with AMD.[23] ORT structures were found in 31 (70.5%) of

Table 1 Demographics and tomographic features of patients with pseudoxanthoma elasticum

Demographics	
Number	52 eyes (27 patients)
Men/women	17/10 (62.9%/37.1%)
Age (years)[a]	65.8 (10.1) (range, 50–89)
Follow-up period (months)[a]	39.5 (18.8) (range, 3–61)
SD-OCT follow-up period (months)[a]	12.6 (9.6) (range, 1–27)
Results of skin biopsy, patient number (%)[b]	26 (96.3%) PXE positive(biopsy was not done for one patient)
Refraction[a]	−1.3 (2.05) (−6.5 to 1.5)
Log MAR BCVA at first SD-OCT visit[a]	0.68 (0.54) (range, −1.8 to 1.6)
Change in log MAR BCVA[a]	0.19 (0.36) (range, −0.33 to 1.3)
Secondary CNV[b]	44 eyes (84.6%)
Tomographic features	
ORT (%)[b]	31 (59.6%)
Location of ORT	
On border of CNV	23 (74.2%)
Over CNV	12 (38.7%)
Cystoid spaces[b]	23 (44.2%)
Bruch's membrane undulation (%)[b]	38 (73.1%)
SRD (%)[b]	7 (13.5%)

Abbreviations: AS, angioid streaks; BCVA, best-corrected visual acuity; CNV, choroidal neovascularization; Log MAR, logarithm of the minimal angle of resolution; ORT, outer retinal tubulation; PXE, pseudoxanthoma elasticum; SRD, serous retinal detachment; SD-OCT, spectral-domain optical coherence tomography.
[a]Values are expressed as means (SD), with the range shown in adjacent parentheses.
[b]Values are the number of eyes, with percentage shown in parenthesis.

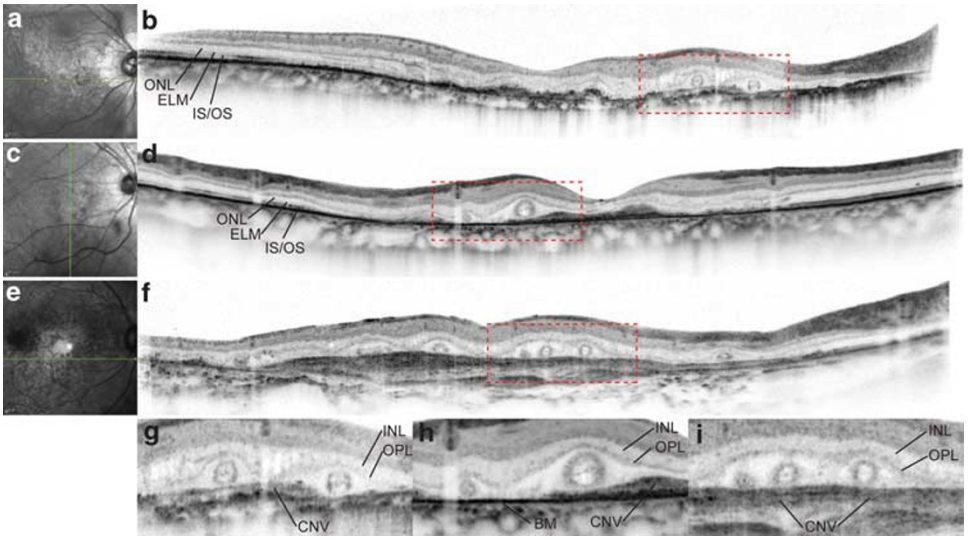

Figure 1 ORT in eyes with CNV secondary to AS and AMD. ORT structures appear to be similar in eyes with CNV secondary to AS (a–d) and AMD (e, f). (a), (c), (e), Infrared images. (b), (d), (f), SD-OCT. The superior and inferior portions of the SD-OCT images in (b), (d), and (f) that did not include retinal images were cropped. Green lines in the infrared images (a, c, e) represent the scan lines for the corresponding SD-OCT images (b, d, f). (g), (h), (i), The magnified ($\times 2$) views of the areas outlined by red dashed lines in the corresponding SD-OCT images (b, d, f). SD-OCT images show characteristic round or ovoid tubular structures (ORTs) in the outer retinas that have highly reflective round/ovoid annular lines. The centres of ORTs contain highly reflective amorphous materials within the annulus. The ORTs were observed at the border of and over the CNV. ELM, external limiting membrane; INL, inner nuclear layer; IS/OS, photoreceptor inner segment/outer segment junction; ONL, outer nuclear layer; OPL, outer plexiform layer.

44 eyes with secondary CNV but were not found in any eye without CNV.

The ORT structures were composed of hyperreflective round/ovoid annular lines (Figure 1). The centres of ORTs were clear or contained highly reflective amorphous materials within the annulus. The vertical diameters of the highly reflective annulus in the SD-OCT images ranged from 68 to 125 μm. The horizontal diameters appeared to be highly variable because they depend on the direction of the OCT scan.

Serial SD-OCT images revealed that the ORT structures formed round structures or short segments in many cases, whereas they formed branching tubular morphology in others. The simultaneous acquisition of FA and SD-OCT images further showed that the some ORTs in the serial SD-OCT images were well correlated with the staining during the late phase of FA that was observed within the CNV in short segments or branching tubule patterns (Figure 2). At the early phase of FA, these tubular structures did not exhibit dye filling as seen in the retinal and choroidal vessels.

Location and photoreceptor damage: The ORT structures appeared to be located beneath the outer plexiform layer (OPL) because they were observed beneath the highly reflective line representing the OPL (Figure 1).

The extent of the ORT structures was determined in relation to the location of the CNV; ORT structures were found at the border of and over the CNV lesions in 23 (74.2%) and 12 (38.7%) of 31 eyes, respectively (Figure 1). However, the ORT was commonly located within the areas where the photoreceptor layer appeared degenerated or in the vicinity of the junction between healthy and degenerated photoreceptor layer. Regardless of the location of the ORT in relation to the CNV, few features representing the integrity of photoreceptor layers were observed, such as the external limiting membrane and the photoreceptor inner and outer segment junction beneath the ORT (Figure 1).

Temporal changes: ORT structures were found before and after anti-CNV treatment in all eyes with AS and secondary CNV that received treatment (26 eyes) during the SD-OCT follow-up. During the follow-up period with serial SD-OCT, ORT structures appeared to remain stable even after anti-CNV treatment.

ORT vs cystoid spaces: Both ORTs and cystoid spaces appeared to be round in shape in SD-OCT images. However, the tomographic features of ORTs and cystoid spaces in speckle noise-reduced SD-OCT images were different. The ORT structures had highly reflective annular margins and were located beneath the OPL hyperreflective band, whereas no cystoid spaces had hyperreflective annular margins and large parts of them were located in the inner nuclear layer or the OPL.

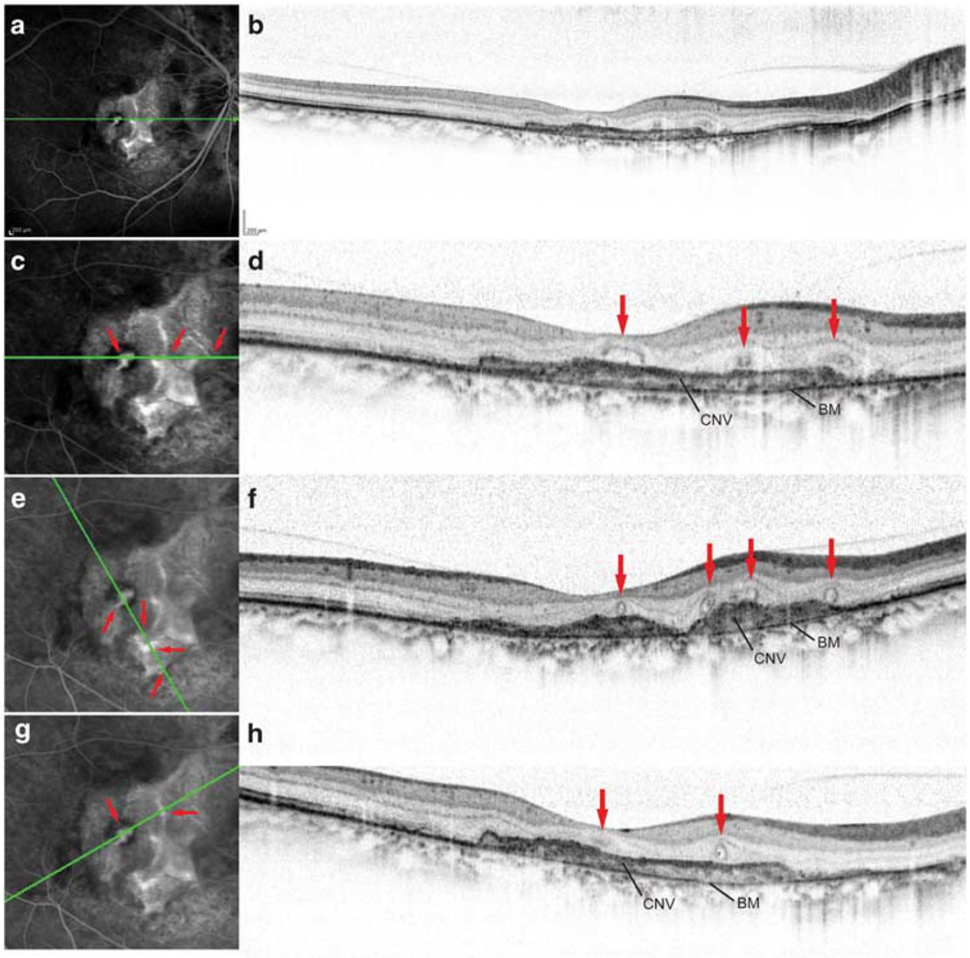

Figure 2 Simultaneous FA and SD-OCT imaging in an eye with CNV secondary to AS (a–h). (a), (c), (e), (g), Late-phase FA image. (b), (d), (f), (h), Speckle noise-reduced SD-OCT. Green lines in the FA images (a, c, e, g) represent the scan lines for the corresponding SD-OCT images (b, d, f, h). In (c), (e), and (g), we magnified ($\times 2$) the FA images by cropping the peripheral portions that did not include the CNV lesions. The corresponding temporal and nasal portions of the SD-OCT images in (d), (f), and (h) were trimmed. The superior and inferior portions of the SD-OCT images were also trimmed to fit the FA images. Simultaneous FA and line scans at various angles indicate the correspondence (red arrows) of the ORT with the faint staining in branching tubule patterns at the late phase of FA that were seen within the CNV.

Simultaneous imaging with FA revealed that the cystoid spaces corresponded to active dye filling in a petaloid or cystic pattern, whereas the ORT structures corresponded to faint staining in short segments or in a branching tubular pattern. Based on the FA images, 23 eyes with AS exhibited cystoid spaces, 13 had a petaloid pattern characteristic to cystoid macular edema, and 10 had cystoid spaces without a petaloid pattern.

Bruch's membrane undulation. SD-OCT imaging enabled us to observe the morphology of Bruch's membrane, particularly in the areas with retinal pigment epithelium degeneration where the remaining Bruch's membrane was directly observable as a highly reflective line (Figure 3). The architecture of the Bruch's membrane in eyes with CNV secondary to AS was unique; the Bruch's membrane did not only exhibit disruption corresponding to the AS in colour fundus photographs but also exhibited repetitively inward and outward deformation, giving it a 'wavy' appearance. We term the former feature 'Bruch's membrane disruptions', and the latter 'Bruch's membrane undulations'. Bruch's membrane undulations were not detected by other imaging modalities including FA, indocyanine green angiography, autofluorescence, and near-infrared reflectance. Bruch's membrane undulations were found in 38 (73.1%) out of a total of 52 eyes, 35 (79.5%) of 44 eyes with CNV and only in 3 (37.5%) of 8 eyes without CNV (Table 1). All of the Bruch's membrane undulations were found beneath the CNV in the macular regions. Some were located within areas with CNV, whereas others partially extended outside those areas. Disruptions in Bruch's

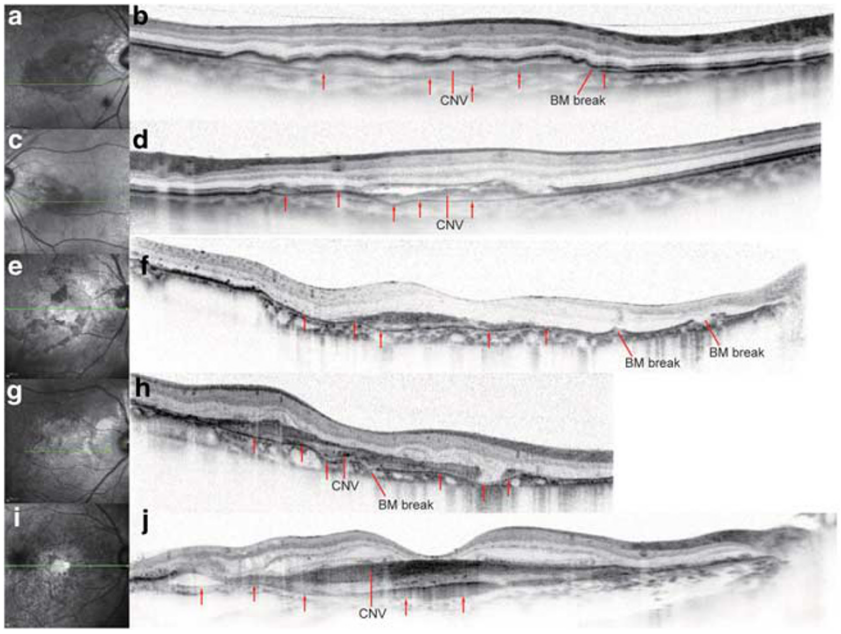

Figure 3 BM undulation in eyes with CNV secondary to angioid streaks AS and AMD (a–j). (a), (c), (e), (g), (i), Infrared images. (b), (d), (f), (h), (j), SD-OCT. The superior and inferior portions of the SD-OCT images in (b), (d), (f), (h), and (j) that did not include retinal images were cropped. The scan length of the SD-OCT image in (h) was 6 mm, whereas it was 9 mm in the other SD-OCT images. Green lines in the infrared images (a, c, e, g, i) represent the scan lines of the corresponding SD-OCT images to the right (b, d, f, h, j). Red arrows indicate BM. The BM undulation was prominent in eyes with CNV secondary to AS (b, d, f, h) but mild, if present at all, in eyes with CNV secondary to AMD (j). BM breaks were found only in eyes with CNV secondary to AS (b, d, f, h).

membrane, which were found in all eyes with AS, were also detected within the areas with CNV on the SD-OCT images.

Comparison of the incidence of tomographic features between eyes with CNV secondary to AS and AMD

The incidence of characteristic tomographic features was compared between 24 eyes from 24 patients with CNV secondary to AS and 44 eyes from 44 patients with CNV secondary to AMD. The demographics of the patients are summarized in Table 2. The patients with CNV secondary to AS were significantly younger ($P<0.0001$) and more myopic ($P=0.027$). There were no significant differences in gender or the logarithm of the minimal angle of resolution best-corrected visual acuity.

The results of the tomographic features are summarized in Table 2. The follow-up duration and number of SD-OCT examinations were not significantly different between groups. During the SD-OCT follow-up, the incidence of ORT was significantly greater in eyes with CNV secondary to AS (70.8%; $P=0.005$) than in eyes with CNV secondary to AMD (34.1%). In the AS group, ORTs were more frequently observed on the border of the CNV in SD-OCT images (76.5%, $P=0.031$) compared with those in the AMD group (33.3%). In contrast, ORTs were less frequently observed over the CNV in the AS group (35.3%, $P=0.042$) compared with those in the AMD group (73.3%). The incidence of Bruch's membrane undulation was significantly greater in eyes with CNV secondary to AS (70.8%; $P<0.0001$) than in eyes with CNV secondary to AMD (11.4%). The features of Bruch's membrane undulation in the SD-OCT images were qualitatively different between groups; the waving pattern in the Bruch's membrane was apparent in the AS group but minimal in the AMD group (Figure 3). We found SRDs only in 16.7% of eyes with CNV secondary to AS but in 59.1% eyes with CNV secondary to AMD; this difference is statistically significant ($P<0.001$). Moreover, the SRDs in the AS group appear to be shallow compared with those in the AMD group. Cystoid spaces were found in 14 (58.3%) of 24 eyes with CNV secondary to AS and in 26 (59.1%) of 44 eyes with CNV secondary to AMD; this difference was not statistically significant (Table 2). No pigment epithelial detachment (PED) was found in eyes with CNV secondary to AS, whereas serous PED was found in 6 (13.6%) of 44 eyes with CNV secondary to AMD (Table 2).

Discussion

In the current retrospective study, we found that, in eyes with CNV secondary to AS, ORTs were more frequently

Table 2 Comparison between eyes with choroidal neovascularization secondary to angioid streaks and age-related macular degeneration

	AS	*AMD*	P-*value*
Demographics			
Number	24 eyes (24 patients)	44 eyes (44 patients)	
Age (years)[a]	66.8 (9.4) (50–89)	75.3 (6.5) (62–85)	<0.0001[b]
Men/women	16/8 (66.7%/33.3%)	29/15 (65.9%/34.1%)	0.789[c]
Refraction (dioptres)[a]	−1.2 (2.15) (−6.75 to 1.5)	0.1 (1.96) (−5.5 to 2.0)	0.027[b]
Log MAR BCVA at first SD-OCT visit[a]	0.747 (0.47) (−0.08 to 1.39)	0.69 (0.46) (−0.08 to 1.70)	0.565[b]
Tomographic features			
SD-OCT follow-up period (months)[a]	13.5 (9.1) (1–27)	11.6 (9.2) (1–29)	0.436
Number. of SD-OCT examinations[a]	4.1 (2.9) (1–13)	4.0 (3.0) (1–11)	0.480[b]
ORT (%)[d]	17 (70.8%)	15 (34.1%)	0.005[c]
Location of ORT			
On border of CNV	13 (76.5%)	5 (33.3%)	0.031[c]
Over CNV	6 (35.3%)	11 (73.3%)	0.042[c]
Cystoid spaces (%)[d]	14 (58.3%)	26 (59.1%)	0.952[c]
Bruch's membrane undulation (%)[d]	17 (70.8%)	5 (11.4%)	<0.0001[c]
SRD (%)[d]	4 (16.7%)	26 (59.1%)	0.001[c]
PED (%)[d]	0	6 (13.6%)	

Abbreviations: AMD, age-related macular degeneration; Log MAR, logarithm of the minimal angle of resolution; No, number; ORT, outer retinal tubulation; SD-OCT, spectral-domain optical coherence tomography; SRD, serous retinal detachment; PED, pigment epithelial detachment.
[a]Values are expressed as means (SD).
[b]Unpaired *t*-test.
[c]Fisher's exact test.
[d]Values are the number of eyes, with percentage shown in parenthesis.

seen and Bruch's membrane undulations were more commonly observed, compared with eyes with CNV secondary to AMD. The incidence of SRD was lower and PED was not seen in eyes with CNV secondary to AS. These differences in tomographic features appear to be useful in facilitating our understanding of the different pathologies between PXE and AMD.

Zweifel *et al*[23] proposed the term 'outer retinal tubulation' (ORT) to describe round- or ovoid-shaped structures on SD-OCT images mainly observed in eyes with AMD. In the present study, the ORT structures found in eyes with PXE were similar to those described in their study in that they had similar round or ovoid appearances with highly reflective annular lines, similar localization in the ONL, and stability over time, even after treatment.

They showed that the incidence of ORT in eyes with AMD was 24.2%.[23] The same authors reported in another report that the ORT was seen in 17 (40.5%) of 42 AS eyes.[22] It is noted that, in the latter study, only 7 (16.7%) eyes had evidence of CNV, indicating that ORT can occur in AS eyes without CNV. In our study, the incidence of ORTs was high (70.8%) in AS eyes with CNV; this incidence was much higher than (34.1%) that in AMD eyes with CNV. This higher incidence of ORT in AS eyes compared with AMD eyes is consistent with the previous studies.[22,23] However, we did not find any ORT structures in AS eyes without CNV in our subjects, inconsistent with the previous studies.[22,23] It is possible that the AS subjects differed with stages and race between studies. In fact, although the previous studies reported that the pattern dystrophy-like changes on fluorescein angiogram and the optic nerve head drusen were observed in a part of study eyes,[21,22] we did not find these fundus features in any subjects. It is uncertain whether the much higher incidence of CNV in our study eyes compared with the previous studies is responsible for some of these differences. The absence of ORT in AS eyes without CNV cannot be fully explained by the high incidence of CNV. Another possibility is that the genetic differences with race causes the variability of the disease phenotype; if this is true, further studies are needed to demonstrate racial differences of fundus features associated with the PXE.

In our study, ORT structures were most frequently found in the vicinity of and over the CNV border in the PXE and AMD groups, respectively. Also, in some eyes, ORTs were observed as faint staining within the CNV during the late phase of FA. Zweifel *et al*[23] speculated that ORT represents a misguided reparative attempt of the photoreceptors and their processes in a 'circling of the wagons' phenomenon. The current study showed the greater incidence of ORT structures and their more frequent localization in the vicinity of the border of the CNV in eyes with AS compared with those with AMD may stem from some of the differences of CNV

development between these two diseases, for example, with respect to the severity, area, and speed of photoreceptor layer damage.

Rosette formation is reported in various animal models, including neural retina leucine zipper (Nrl) knockout and Pax6 overexpression mice, and in models of retina transplantation.[24–27] In the retina of Nrl knockout mice, Fischer *et al*[24] show that the histology of rosette structures corresponds with the round or ovoid features with highly reflective annular lines observed in speckle noise-reduced SD-OCT. Although it remains unclear whether the rosettes in animal models are same as the ORT in human patients,[26] this correspondence suggests that the ORT is comprised of rearranged neuronal cells. Unfortunately, histopathological evidence that supports the presence and contents of ORT structures in patients' eyes is limited. We found rosette structures in eyes with AS and AMD in a few light microscope sections.[28] These structures are actually comprised of circularly arranged photoreceptors containing a single or a few cells inside and were observed immediately anterior to the retinal pigment epithelium. Taken together, the interpretation of the ORT as a photoreceptor rosette appears to be appropriate.

Bruch's membrane undulation appears to be characteristic in eyes with CNV secondary to AS because it occurred six times more frequently compared with eyes with CNV secondary to AMD. In AMD, Bruch's membrane undulations were, if present at all, less prominent. In their presentation of the tomographic features of patients with PXE, Charbel Issa *et al*[21] focused on the variable disruptions of the Bruch's membrane, including smaller and larger breaks with displaced edges or fibrous tissue growing within it, as well as its degradation into pieces. In our study, although we found similar variable disruptions and degradation of the Bruch's membrane, we additionally focused on the undulations because this feature appears to be closely associated with the underlying causes of PXE lesions; progressive fragmentation and calcification of the elastic fibres in the Bruch's membrane appear to make it weak.[1,2] The undulations likely represent the weak integrity of the Bruch's membrane.

The wavy architecture, breaks, and the dislocation of fragmented pieces of the Bruch's membrane have been shown in previous histopathological studies.[28,29] Although it was unclear whether these minute pathologies are real, or artifacts resulting from postmortem changes, and histological fixation, noninvasive SD-OCT imaging revealed that this characteristic feature of the Bruch's membrane are in fact a real finding.

In our subjects, the incidence of SRDs was significantly lower in eyes with CNV secondary to AS (15.9%) compared with eyes with CNV secondary to AMD (54.5%) during follow-up by SD-OCT. Ozawa *et al*[30] found SRDs in 53% of eyes with exudative AMD. Zweifel *et al*[22] found SRDs in 33.3% of AS eyes; they showed that the SRDs were not only associated with leakage from CNV, but also with pattern dystrophy-like findings. As mentioned above, pattern dystrophy-like findings were not observed in our study. Thus, active leakage from CNV may less frequently occur in AS eyes compared with AMD eyes.

A limitation of this study is the variable subject conditions, particularly therapeutic conditions, which stem from its retrospective cohort design. Another limitation is that our study included only Japanese subjects, which may limit the interpretation of the results. However, this limitation provides a simpler study population not affected by ethnic differences, which may be beneficial for comparing SD-OCT features between AS eyes and AMD eyes.

Conclusion

In conclusion, speckle noise-reduced SD-OCT imaging clearly revealed a high incidence of ORTs and Bruch's membrane undulation in Japanese eyes with PXE. The incidence of these features was much higher in AS eyes with CNV than AMD eyes with CNV; the incidence of SRD was also much lower. Thus, SD-OCT imaging allows the characterization of unique fundus lesions characteristic to AS.

Summary

What was known before

- Angioid streaks (AS) is a rare disorder and leads to severe vision loss when CNV develops.
- AS occurs as irregular crack-like dehiscence in the Bruch's membrane (BM) and SD-OCT show disruptions in BM corresponding to those breaks.
- SD-OCT shows an unique tomographic feature, outer retinal tabulation (ORT), in eyes with AS.

What this study adds

- SD-OCT revealed a greater incidence of ORT in eyes with CNV secondary to AS compared with eyes with CNV secondary to age-related macular degeneration (AMD).
- SD-OCT also revealed repetitive inward and outward deformation of Bruch's membrane, giving it a 'wavy' appearance in AS eyes with CNV. This unique feature was in AMD eyes with CNV.

Conflict of interest

Masanori Hangai is a paid advisory board member for NIDEK, and received consulting fees from Topcon,

lecture fees from Heidelberg Engineering and Santen. Yoshimura Nagahisa is a paid advisory board member for NIDEK, lecture fees from Nidek, Topcon, and Canon, and research funding from Topcon, Nidek, and Canon. The other authors declare no conflict of interest.

References

1 Hu X, Plomp AS, van Soest S, Wijnholds J, de Jong PT, Bergen AA. Pseudoxanthoma elasticum: a clinical, histopathological, and molecular update. *Surv Ophthalmol* 2003; **48**: 424–438.
2 Le Saux O, Urban Z, Tschuch C, Csiszar K, Bacchelli B, Quaglino D *et al*. Mutations in a gene encoding an ABC transporter cause pseudoxanthoma elasticum. *Nat Genet* 2000; **25**: 223–227.
3 Finger RP, Charbel Issa P, Ladewig MS, Gotting C, Szliska C, Scholl HP *et al*. Pseudoxanthoma elasticum: genetics, clinical manifestations and therapeutic approaches. *Surv Ophthalmol* 2009; **54**: 272–285.
4 Mimoun G, Tilleul J, Leys A, Coscas G, Soubrane G, Souied EH. Intravitreal ranibizumab for choroidal neovascularization in angioid streaks. *Am J Ophthalmol* 2010; **150**: 692–700.
5 Sawa M, Gomi F, Tsujikawa M, Sakaguchi H, Tano Y. Long-term results of intravitreal bevacizumab injection for choroidal neovascularization secondary to angioid streaks. *Am J Ophthalmol* 2009; **148**: 584–590.
6 Dreyer R, Green WR. The pathology of angioid streaks: a study of twenty-one cases. *Trans Pa Acad Ophthalmol Otolaryngol* 1978; **31**: 158–167.
7 Clarkson JG, Altman RD. Angioid streaks. *Surv Ophthalmol* 1982; **26**: 235–246.
8 Connor PJ Jr., Juergens JL, Perry HO, Hollenhorst RW, Edwards JE. Pseudoxanthoma elasticum and angioid streaks. A review of 106 cases. *Am J Med* 1961; **30**: 537–543.
9 Dabbs TR, Skjodt K. Prevalence of angioid streaks and other ocular complications of Paget's disease of bone. *Br J Ophthalmol* 1990; **74**: 579–582.
10 Mansour AM, Shields JA, Annesley Jr WH, el-Baba F, Tasman W, Tomer TL. Macular degeneration in angioid streaks. *Ophthalmologica* 1988; **197**: 36–41.
11 Shields JA, Federman JL, Tomer TL, Annesley WH Jr. Angioid streaks. I. Ophthalmoscopic variations and diagnostic problems. *Br J Ophthalmol* 1975; **59**: 257–266.
12 Lim JI, Bressler NM, Marsh MJ, Bressler SB. Laser treatment of choroidal neovascularization in patients with angioid streaks. *Am J Ophthalmol* 1993; **116**: 414–423.
13 Brancato R, Menchini U, Pece A, Davi G, Capoferri C. Laser treatment of macular subretinal neovascularizations in angioid streaks. *Ophthalmologica* 1987; **195**: 84–87.
14 Ozdek S, Bozan E, Gurelik G, Hasanreisoglu B. Transpupillary thermotherapy for the treatment of choroidal neovascularization secondary to angioid streaks. *Can J Ophthalmol* 2007; **42**: 95–100.
15 Aras C, Baserer T, Yolar M, Yetik H, Artunay O, Guzel H *et al*. Two cases of choroidal neovascularization treated with transpupillary thermotherapy in angioid streaks. *Retina* 2004; **24**: 801–803.
16 Bhatnagar P, Freund KB, Spaide RF, Klancnik Jr JM, Cooney MJ, Ho I *et al*. Intravitreal bevacizumab for the management of choroidal neovascularization in pseudoxanthoma elasticum. *Retina* 2007; **27**: 897–902.
17 Karacorlu M, Karacorlu S, Ozdemir H, Mat C. Photodynamic therapy with verteporfin for choroidal neovascularization in patients with angioid streaks. *Am J Ophthalmol* 2002; **134**: 360–366.
18 Menchini U, Virgili G, Introini U, Bandello F, Ambesi-Impiombato M, Pece A *et al*. Outcome of choroidal neovascularization in angioid streaks after photodynamic therapy. *Retina* 2004; **24**: 763–771.
19 Sakamoto A, Hangai M, Yoshimura N. Spectral-domain optical coherence tomography with multiple B-scan averaging for enhanced imaging of retinal diseases. *Ophthalmology* 2008; **115**: 1071–1078.
20 Hangai M, Yamamoto M, Sakamoto A, Yoshimura N. Ultrahigh-resolution versus speckle noise-reduction in spectral-domain optical coherence tomography. *Opt Express* 2009; **17**: 4221–4235.
21 Charbel Issa P, Finger RP, Holz FG, Scholl HP. Multimodal imaging including spectral domain OCT and confocal near infrared reflectance for characterization of outer retinal pathology in pseudoxanthoma elasticum. *Invest Ophthalmol Vis Sci* 2009; **50**: 5913–5918.
22 Zweifel SA, Imamura Y, Freund KB, Spaide RF. Multimodal fundus imaging of pseudoxanthoma elasticum. *Retina* 2011; **31**: 482–491.
23 Zweifel SA, Engelbert M, Laud K, Margolis R, Spaide RF, Freund KB. Outer retinal tubulation: a novel optical coherence tomography finding. *Arch Ophthalmol* 2009; **127**: 1596–1602.
24 Fischer MD, Huber G, Beck SC, Tanimoto N, Muehlfriedel R, Fahl E *et al*. Noninvasive, *in vivo* assessment of mouse retinal structure using optical coherence tomography. *PLoS One* 2009; **4**: e7507.
25 Wenzel A, von Lintig J, Oberhauser V, Tanimoto N, Grimm C, Seeliger MW. RPE65 is essential for the function of cone photoreceptors in NRL-deficient mice. *Invest Ophthalmol Vis Sci* 2007; **48**: 534–542.
26 Nikonov SS, Daniele LL, Zhu X, Craft CM, Swaroop A, Pugh EN Jr.. Photoreceptors of Nrl -/- mice coexpress functional S- and M-cone opsins having distinct inactivation mechanisms. *J Gen Physiol* 2005; **125**: 287–304.
27 Daniele LL, Lillo C, Lyubarsky AL, Nikonov SS, Philp N, Mears AJ *et al*. Cone-like morphological, molecular, and electrophysiological features of the photoreceptors of the Nrl knockout mouse. *Invest Ophthalmol Vis Sci* 2005; **46**: 2156–2167.
28 Green WR. *Ophthalmic Pathology: An Atlas and Textbook*. Saunders: Philadelphia, 1996.
29 Hagedoorn A. Angioid streaks. *Arch Ophthalmol* 1939; **21**: 746–774.
30 Ozawa S, Ishikawa K, Ito Y, Nishihara H, Yamakoshi T, Hatta Y *et al*. Differences in macular morphology between polypoidal choroidal vasculopathy and exudative age-related macular degeneration detected by optical coherence tomography. *Retina* 2009; **29**: 793–802.